

Baicalin attenuates LPS-induced alveolar type II epithelial cell A549 injury by attenuation of the FSTLI signaling pathway via increasing miR-200b-3p expression

Innate Immunity
2021, Vol. 27(4) 294–312
© The Author(s) 2021
Article reuse guidelines:
sagepub.com/journals-permissions
DOI: 10.1177/17534259211013887
journals.sagepub.com/home/ini



Xin-ya Duan^{1,*}, Yang Sun^{2,*}, Zhu-feng Zhao³, Yao-qing Shi³,
Xun-yan Ma³, Li Tao³ and Ming-wei Liu³

Abstract

In China, baicalin is the main active component of *Scutellaria baicalensis*, which has been used in the treatment of inflammation-related diseases, such as inflammation-induced acute lung injury. However, its specific mechanism remains unclear. This study examined the protective effect of baicalin on LPS-induced inflammation injury of alveolar epithelial cell line A549 and explored its protective mechanism. Compared with the LPS-induced group, the proliferation inhibition rates of alveolar type II epithelial cell line A549 intervened by different concentrations of baicalin decreased significantly, as did the levels of inflammatory factors IL-6, IL-1 β , prostaglandin 2 and TNF- α in the supernatant. The expression levels of inflammatory proteins inducible NO synthase (iNOS), NF- κ B65, phosphorylated ERK (p-ERK1/2), and phosphorylated c-Jun N-terminal kinase (p-JNK1) significantly decreased, as did the protein expression of follistatin-like protein 1 (FSTLI). In contrast, expression of miR-200b-3p significantly increased in a dose-dependent manner. These results suggested that baicalin could significantly inhibit the expression of inflammation-related proteins and improve LPS-induced inflammatory injury in alveolar type II epithelial cells. The mechanism may be related to the inhibition of ERK/JNK inflammatory pathway activation by increasing the expression of miR-200b-3p. Thus, FSTLI is the regulatory target of miR-200b-3p.

Keywords

Baicalin, alveolar type II epithelial cells, inflammatory response, miR-200b-3p, FSTLI

Date received: 29 October 2020; revised: 7 April 2021; accepted: 12 April 2021

Introduction

Sepsis is a fatal organ dysfunction caused by infection-induced host reaction disorder.¹ About 31.5 million sepsis cases and 19.4 million severe sepsis cases have been reported worldwide, resulting in a death toll as high as 5.3 million every year.² The lungs are the most vulnerable target organ of sepsis. About 25–50% of sepsis cases might develop into acute lung injury (ALI) or even acute respiratory distress syndrome.³ In complicated organ dysfunction, ALI has the earliest occurrence and the highest incidence rate.⁴ The pathological basis of ALI includes excessive persistent alveolar inflammation accompanied with alveolar epithelial cell damage or even apoptosis. At present,

¹Department of Tuberculosis Diseases, Third People's Hospital of Kunming City, China

²Department of Nephrology, The Sixth Affiliated Hospital of Kunming Medical University, China

³Department of Emergency Medicine, First Affiliated Hospital of Kunming Medical University, China

*The authors contributed equally to this research.

Corresponding author:

Ming-wei Liu, Department of Emergency Medicine, First Affiliated Hospital of Kunming Medical University, 295 Xichang Road, Wuhua District, Kunming, Yunnan Province, 650032, China.
Email: lmw2004210@163.com



ALI caused by sepsis is still treated with anti-infection, respiratory support, immune regulation, and symptomatic support; its death rate can reach as high as 70%.^{5,6} Therefore, searching for new therapeutic targets and effective drugs may be helpful to reduce the death rate of sepsis-induced ALI.

Follistatin-like protein 1 (FSTL1), also known as TGF- β -stimulated clone 36 (TSC-36) or follistatin-related protein (FRP), is an extracellular matrix protein and a secretory glycoprotein with molecular mass of about 35,000 Da.⁷ FSTL1 is involved in the occurrence and development of many diseases and is closely related to autoimmune diseases, tumor occurrence and metastasis, and cardiovascular diseases such as heart development, myocardial ischemia, cardiac hypertrophy, angiogenesis, and mitral valve disease.^{8–11} Studies have found that FSTL1 is highly expressed in the serum of patients with rheumatoid arthritis, osteoarthritis, and Sjogren's syndrome.^{12–14} In rheumatoid arthritis, FSTL1 can promote the secretion of pro-inflammatory cytokines IFN- γ , TNF- α , IL-1 β , and IL-6 and induce synovitis and inflammatory cell infiltration in synovium and surrounding tissues.¹⁵ The overexpression of FSTL1 in monocytes and macrophages cultured *in vitro* and septic shock in mice can induce the expression of caspase-1 and NLRP3, thereby confirming that FSTL1 can mediate the occurrence of pro-inflammatory events.¹⁶ FSTL1 can promote the inflammatory response through signaling pathways such as ERK1/2, IKK β , I κ B- α , JNK, and NF- κ B.¹⁷

Scutellaria baicalensis is a traditional Chinese medicine with a long history. Its effects include clearing away heat and drying dampness, purging fire for removing toxins, and preventing hemostasis and miscarriage. Baicalin is one of the main effective components of *S. baicalensis*, which features good anti-inflammatory, antioxidant, and anti-apoptosis activities. Baicalin can attenuate myocardial ischemia or reperfusion injury through multiple signaling pathways after inhibiting 12/15-lipoxygenase.¹⁸ It can also attenuate hepatic and renal injury caused by myocardial ischemia/reperfusion injury.^{19,20} Baicalin can prevent cisplatin-induced acute renal injury by down-regulating the activities of MAPKs and the NF- κ B pathway and increasing the production of antioxidants.²¹ Recent studies have found that baicalin can alleviate the inflammatory response by inhibiting the TLR4-mediated NF- κ B and MAPK signaling pathways in an LPS-induced mice mastitis model.²² Baicalin can attenuate oxLDL-induced oxidative stress and inflammatory response by regulating the expression of AMPK- α .²³

MicroRNA (miRNA) is a series of endogenous non-coding small RNAs with a length of 19–22 nucleic acids. It is cut from the double-stranded RNA precursor with hairpin structures. It has high conservation, expression

sequence, and tissue specificity. By binding with the 3'-untranslated region (3'-UTR) of the Zen gene miRNA, miRNA inhibits OPG translation at the post-transcriptional level to achieve negative regulation of gene expression. miRNA has a wide range of influence on different molecular signaling pathways; it is closely related to cell proliferation, differentiation, and apoptosis, making it important for the growth and development of animals and plants, tissue differentiation, and disease occurrence.²⁴ An increasing number of studies have adopted miRNAs as targets or therapeutic targets for disease detection.²⁵ In the inflammatory response, different miRNAs may promote or inhibit inflammation.²⁶ In the differentiation process from monocyte into macrophages, miR-223, miR-15a, and miR-16 jointly regulate IKK α . When their expression levels decrease, IKK α phosphorylation increases and activates NF- κ B.^{27,28} In the peripheral blood mononuclear cells of patients with type 1 diabetes, overexpression of miR-885-3p can inhibit the inflammatory response of mononuclear cells by regulating the activity of the TLR4/NF- κ B signaling pathway.²⁹ However, the inflammation regulating mechanism of miRNAs remains unclear.

MiR-200b-3p is a member of the miR-200 family, which is involved in a variety of biological events, such as angiogenesis, cell migration, organ fibrosis, and regulation of inflammatory factor secretion.^{30–33} Studies have shown that the expression of miR-200b significantly decreases in mucosal lesions at the acute stage of ulcerative colitis. Overexpression of miR-200b *in vitro* can promote IEC proliferation, reduce the IEC inflammatory response, inhibit epithelial–mesenchymal transition (EMT) of IEC, and improve intestinal epithelial barrier function through the transepithelial cell pathway.³⁴ The expression of miR-200b-3p in HCMV-infected tissues decreases and is negatively correlated with inflammation and viral load of the lesion.³⁵ However, the specific mechanism is unclear. The ERK/JNK signaling pathway is an important inflammation regulation pathway.²⁹ In this experiment, we predicted that FSTL1 was the regulatory target of miR-200b-3p using TargetScan software. Therefore, we hypothesized that miR-200b-3p played an important role in the occurrence and development of endotoxin-induced ALI. We further explored whether baicalin can improve endotoxin-induced ALI by increasing the expression of miR-200b-3p and decreasing the activity of FSTL1 and the ERK/JNK signaling pathway.

Material and methods

Materials and reagents

Baicalin was obtained from Nanjing Jingzhu Biotechnology Co., Ltd. (batch no.: 21967-41-9,

purity 95%). Alveolar type II epithelial cells (A549 cell line) were provided by Shanghai Sixin Technology Biological Co., Ltd. (sourced from US ATCC Cell Bank). FBS and 1640 medium were purchased from US Gibco Company. Trypsin was purchased from US Thermo Scientific Company. CCK8 kits were purchased from Beijing Zhijie Fangyuan Technology Co., Ltd. LPS was from Abcam Company (UK). ELISA kits of IL-6, IL-1 β , prostaglandin 2 (PGE2), and TNF- α were purchased from Wuhan Huamei Biological Co., Ltd. Rabbit anti-mouse β -actin, NF- κ B65, p-I κ B- α , I κ B- α , FSTL1, ERK1/2, and JNK1 primary Abs were all purchased from UK Abcam Company. HRP-labeled IgG secondary Ab was purchased from Wuhan Guge Biology Co., Ltd.

A549 cell culture and group

In this study, 1640 medium containing 10% FBS was used to culture A549 cells. When A549 cells grew and fused to 70%, they were seeded into the culture dish at the density of 1×10^4 /ml per well plate and cultured in a 5% CO₂ incubator at 37°C. They were digested with 0.25% trypsin and passaged at 1:2 after 7 d of culture. The cells were inoculated in a 25 cm² culture flask with a density of 1×10^5 cells/ml. When the fusion rate reached 60%, the cells were synchronized to grow for 24 h and then divided into different groups. To observe the effect of LPS on the activity and proliferation of A549 cells, according to a previously described technique,²² we added different concentrations of LPS (0.5, 1.0, 1.5, and 2.0 mg/l) for 24 h. To observe the effect of baicalin on endotoxin-induced A549 cell injury, the cells were divided into the control group, LPS-induced group, LPS + 10 μ mol/l baicalin group, LPS + 25 μ mol/l baicalin group, LPS + 50 μ mol/l baicalin group, and LPS + 75 μ mol/l baicalin group. As previously described,¹⁹ we first added different concentrations of baicalin (10–75 μ M) and cultured the cells for 2 h. Second, we added LPS (1.0 μ M) solution and cultured the cells for 24 h. Finally, we determined the indicators.

Analysis of cell viability

The proliferation activities of A549 cells in different groups were measured by using a CCK-8 kit (CCK-8, Qi Hai Biology). A549 cells were seeded on a 96-well plate. After cells were fused to 70%, they were moved to serum-free medium. After treatment with different conditions, 10 μ l of CCK-8 solution was added into each well and incubated in the dark for 2–4 h. The absorbance values (A450 nm) were measured at 450 nm by using an enzyme-labeled instrument.

Cell transfection

An appropriate amount of A549 cells at the logarithmic phase was inoculated into a six-well plate. When the cells grew overnight and adhered to the wall until 60%, miR-200b-3p mimic, miR-200b-3p inhibitor, mimic control, and inhibitor control were transfected into A549 cells following the operation instructions of Lipofectamine 2000 transfection reagent. The transfection concentration was 50 nmol/l. After transfecting for 6 h, the cells were moved to fresh medium and cultured for another 24 h. The cells were then collected for RT-PCR and Western blot analyses.

Determination of cell survival

The liquid in each well of the 96-well plate was removed. About 270 μ l of DMEM and 30 μ l of 5g/l MTT working solution were added and mixed. After incubation at 37°C for 4 h, the culture medium in the well was discarded, and 270 μ l of DMSO was added into each well. The solution was fully dissolved after shaking for 10 min. The OD values of each well were measured at 490 nm by using an enzyme-labeled instrument. Compared with the OD value of the control group, the cell survival rate of each well (%) = OD value of each well/mean OD value of the control group \times 100 was calculated.⁵

Cell morphology

The cell morphology of A549 cells in different groups was detected by using the AO/EB method. A549 cells were seeded on a 96-well plate. After cells were fused to 70%, they were moved to serum-free medium. After treatment with different conditions, a working solution of AO solution: EB solution = 1:1 was prepared. About 20 μ l of working solution was added to each well and left at room temperature (37°C) for 5 min. Finally, the cells were observed under a fluorescent inverted microscope, and images were obtained.

Flow cytometric detection of the apoptotic rate of A549 cells

The A549 cells were washed with pre-cooled PBS and suspended with 300 μ l of buffer solution. The cell concentration was adjusted to 1×10^6 /ml, and 100 μ l was placed in a flow tube. About 5 μ l of ANNEXIN V-FITC (BD Pharmingen, San Diego, CA, USA) and 5 μ l of PI (Abcam, Cambridge, MA, USA) were added to the tube, incubated at room temperature for 15 min, and added with 400 μ l of PBS to detect cell apoptosis through flow cytometry. Apoptotic cells were quantified as the percentage of cells stained with Annexin V.

Table 1. Primer sequences of RT-PCR analysis.

Gene	Primer	Product(bp)
miR-200b-3p	F-5'-GCGGGCTAATACTGCCTGG -3' R-5'-ATCCAGTCCAGGGTCCGAAA-3'	218 bp
U6	F-5'-CTCGCTTCGGCAGCACA-3' R-5'-AACGCTTCACGAATTTGCGT-3'	194 bp
FSTL1 mRNA	F-5'-TTATGATGGGCAGGCAAAGAA-3' R-5'-ACTGCCTTTAGAGAACCAGCC-3'	183 bp
ERK1 mRNA	F-5'-AGGCATCCGAGACATCCTC -3' R-5'-CGGTCAGAAAGCCAGTGTG-3'	217 bp
JNK1 mRNA	F-5'-GCCCGATGAAACCTCGCAGAT -3' R-5'-ACGCAGGCAATCCTACTGGA-3'	218 bp
β -Actin	F-5'-ATGGTGAAGGTCGGTGTG-3' R-5'-AACTTGCCGTGGGTAGAG-3'	154 bp

Target gene prediction

Target gene prediction software such as miR-Base (<http://www.mirbase.org/>), TargetScan (<http://www.targetscan.org/>), and PicTar (<http://pictar.mdc-berlin.de/>) were used to predict the target gene of miR-200b-3p, which may be FSTL1. Wild type (WT)-FSTL1 and mutant (MUT)-FSTL1 luciferase gene vectors were constructed by conventional methods. The two plasmids were mixed with miR-200b-3p mimics, miR-200b-3p inhibitor, mimic control, and inhibitor control and then co-transfected into A549 cells, which were recorded as Wt+miR-200b-3p mimics, Mut+miR-200b-3p, Wt+negative control, and Mut+negative control, respectively. After incubation in a 5% CO₂ incubator at 37°C for 48 h, the activities of dual luciferase were measured by dual luciferase reporter gene kits. The level of FSTL1 in A549 cells with overexpression of miR-200b-3p was detected by RT-PCR and Western blot.

Real-time quantitative PCR

A549 cells in the treatment group were collected. The cell RNA was extracted by a total RNA extraction kit and reverse transcribed into cDNA following the PrimeScript™ RT reagent kit. The expression levels of FSTL1, ERK1, JNK1 mRNA, and miR-200b-3p were measured by real-time PCR. The reaction system was as follows: SYBR Premix Ex Taq™ II (10 μ l), PCR primer (2 μ l), DNA template (2 μ l), DEPC water (6 μ l), and total reaction system (20 μ l). Each sample was set with three parallel multiple pores, and the reaction system was completed by a PCR instrument. To detect the level of miR-200b-3p, we used a TaqMan MicroRNA Assay Kit (Applied Biosystems, Foster City, CA, USA) to determine the expression level of miR-200b-3p by the $2^{-\Delta\Delta Ct}$ method. Reaction conditions were as follows: pre-denaturation at 95°C for 30 s, reaction at 95°C for 5 s, and annealing

at 60°C for 30 s for 40 cycles. The primer series are shown in Table 1.

U6 was used as the internal reference for miR-200b-3p, and β -actin was used as the internal reference for the expression of the FSTL1, ERK1, and JNK1 genes. After the reaction, the cycle threshold (CT) of each gene was calculated and compared with the reference gene U6 to determine the expression level.

Western blot analysis

The cell lysis solution, protease inhibitor, and phosphatase inhibitor were mixed at the ratio of 8:1:1 to produce cell lysis buffer. About 150 μ l of RIPA cell lysis buffer was added into each well, and the cells were lysed for 30 min in an ice bath to extract the total cellular protein of each group. After centrifugation at 4°C for 15 min, the purity of protein was detected by using a BCA protein quantitative kit. About 50 μ g of protein extraction solution was electrophoretically separated by 10% SDS-PAGE and then incubated with 5% defatted milk for 1.5 h. NF- κ B65, p-I κ B- α , I κ B- α , β -actin, FSTL1, and ERK1/2 primary Ab (1:1000) were correspondingly added at 4°C for the whole night. The next day, the membrane was washed with TBST three times, and HRP-labeled IgG (volume dilution ratio at 1:3000) was added. After reacting at room temperature for 1 h, the membrane was washed with TBST three times again for 10 min each time. ECL chemiluminescence solution was added for color development. The gray value of the strip was analyzed by Image lab software, and β -actin was used as an internal reference.

Determination of inflammatory factors of A549

Cells in the logarithmic growth phase were digested, resuspended, and inoculated on six plates. After cells grew by adhering to the wall, the old culture medium was removed. After culturing cells of different groups

for 24 h, the cells and cell supernatant were collected. The inflammatory factors PGE2, IL-6, IL-1 β , and TNF- α were detected by using an ELISA kit. The operation steps were strictly in accordance with the instruction book.

Statistical analysis

GraphPad Prism 6 was used for statistical analysis. The experimental data was represented as mean \pm standard deviation. One-way ANOVA was used for comparison among groups. The LSD method was used for pairwise significant comparison between groups. $P < 0.05$ was considered statistically significant.

Results

LPS attenuated the cell viability and survival of alveolar type II A549 cells

To observe the effect of LPS on the cell viability and survival rate of alveolar A549 cells, we incubated the cells with various concentrations of LPS (0.5, 1.0, 1.5, and 2.0 mg/l) for 24 h. A549 cell viability was measured using CCK-8, and the proliferation rate was measured by the MTT assay. LPS attenuated the cell viability and survival rate of A549 cells in a concentration-dependent manner (Figure 1). Concentrations as low as 1.0 mg/l LPS were effective in decreasing the cell viability and survival rate of A549 cells.

LPS increased the inflammation of alveolar type II epithelial cells

To investigate the effect of LPS on the inflammation of alveolar type II epithelial cells, we incubated A549 cells with various concentrations of LPS (0.25, 0.5, 1.0, 1.5, and 2.0 mg/l) for 24 h. IL-6, PGE2, IL-1 β , and TNF- α in A549 cells were measured by ELISA. LPS increased

the levels of IL-6, IL-1 β , and TNF- α in A549 cells in a concentration-dependent manner (Figure 2). LPS at concentrations as low as 1.0 μ M was effective in increasing IL-6, IL-1 β , and TNF- α levels in A549 cells.

LPS increased the activity of the FSTL1 and ERK/JNK signaling pathway in alveolar type II epithelial cells

To evaluate the effect of LPS on the FSTL1 and ERK/JNK signaling pathway in A549 cells, we incubated A549 cells with various concentrations of LPS (0.5, 1.0, 1.5, and 2.0 μ M) for 24 h. The expression levels of FSTL1, p-JNK1, p-ERK1/2, NF- κ B65, p-I κ B- α , iNOS, and COX-2 proteins were measured by Western blot analysis. LPS increased the expression levels of FSTL1, p-JNK1, p-ERK1/2, NF- κ B65, p-I κ B- α , iNOS, and COX-2 proteins in A549 cells in a concentration-dependent manner (Figure 3). LPS at concentrations as low as 1.0 μ M was effective in increasing the activity of the FSTL1 and ERK/JNK signaling pathway in A549 cells.

Effect of miR-200b-3p mimic on miR-200b-3p, FSTL1, ERK, and JNK1 mRNA in LPS-induced alveolar type II epithelial cells

The A549 cells were transfected with miR-200b-3p mimic and miR-200b-3p inhibitor in the presence of 1 mg/l LPS for 24 h. miR-200b-3p, FSTL1, ERK, and JNK1 mRNA expression in LPS-induced alveolar type II epithelial cells was measured by RT-PCR. As shown in Figure 4, miR-200b-3p mimic increased miR-200b-3p expression and decreased FSTL1, ERK, and JNK1 mRNA expression. miR-200b-3p inhibitor attenuated miR-200b-3p expression and increased FSTL1, ERK, and JNK1 mRNA expression in LPS-induced A549 cells.

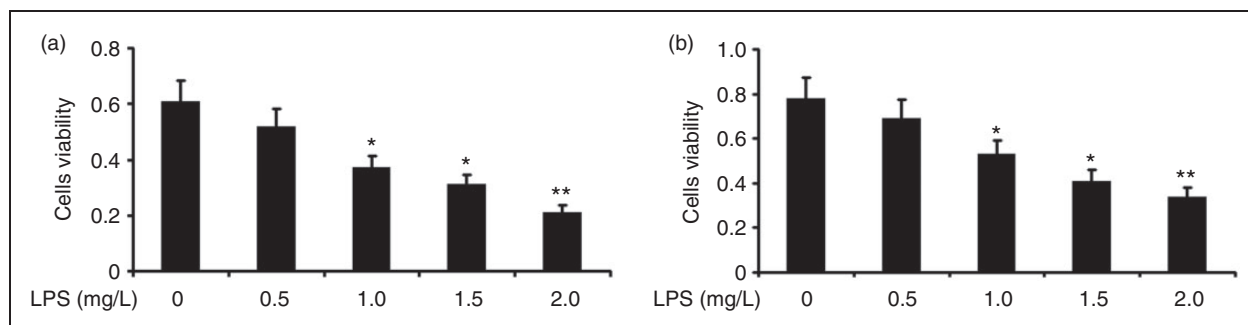


Figure 1. Effect of LPS on the cell viability and survival rate of alveolar type II epithelial cells. After A549 cells were incubated with various concentrations of LPS (0.5, 1.0, 1.5, and 2.0 mg/l) for 24 h, their cell viability was measured using CCK-8. The survival rate was then measured by the MTT assay. The data from three independent experiments are presented as the mean \pm SEM. * $P < 0.05$, ** $P < 0.01$ versus the control group. $P < 0.05$, the LPS (1.5 mg/l) group versus the LPS (1.5 mg/l) group and the LPS (2.0 mg/l) group. $P > 0.05$, the LPS (1.5 mg/l) group versus the LPS (2.0 mg/l) group.

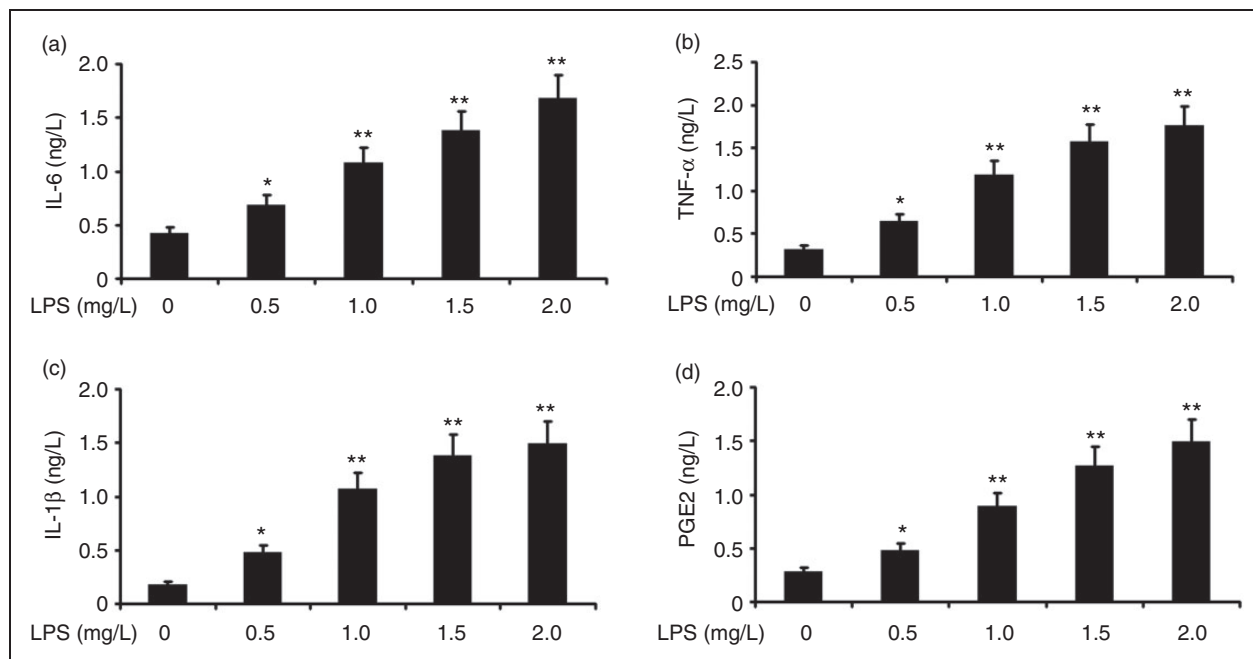


Figure 2. Effect of LPS on the inflammation of alveolar type II epithelial cells. A549 cells were incubated with various concentrations of LPS (0.5, 1.0, 1.5, and 2.0 mg/l) for 24 h. IL-6, IL-1β, PGE2, and TNF-α in A549 cells were measured by ELISA. The data from three independent experiments is presented as the mean ± SEM. * $P < 0.05$, ** $P < 0.01$ versus the control group. $P < 0.05$, the LPS (1.5 mg/l) group versus the LPS (1.5 mg/l) group and the LPS (2.0 mg/l) group. $P > 0.05$, the LPS (1.5 mg/l) group versus the LPS (2.0 mg/l) group.

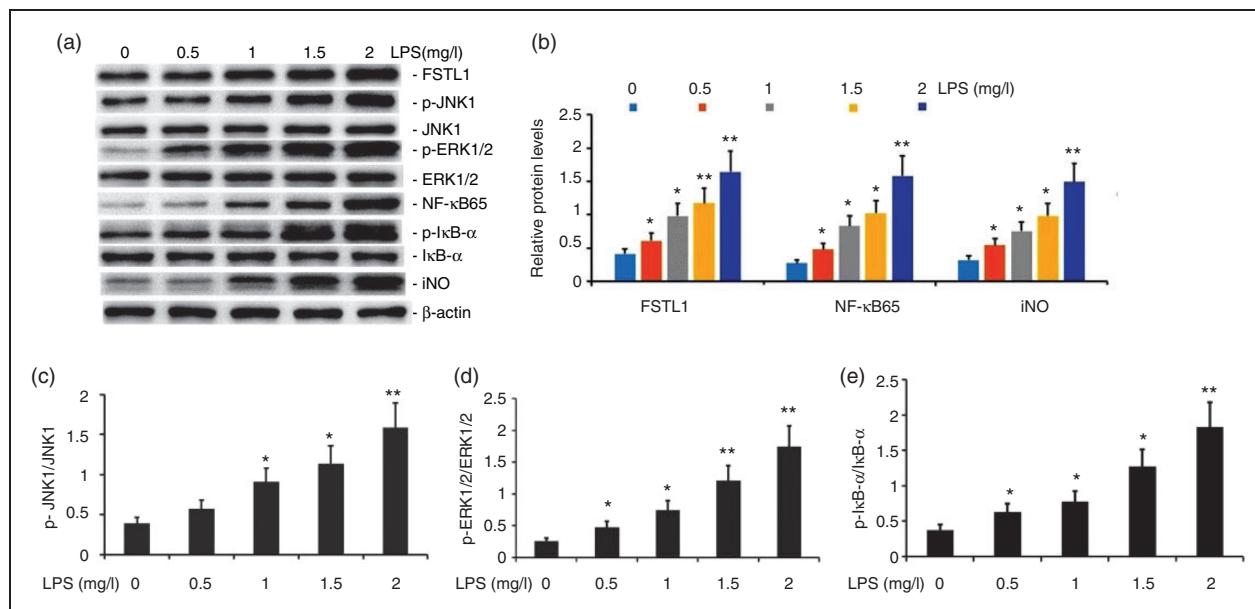


Figure 3. Effect of LPS on the activity of the FSTL1 and ERK/JNK signaling pathway in A549 cells. A549 cells were incubated with various concentrations of LPS (0.5, 1.0, 1.5, and 2.0 mg/l) for 24 h. FSTL1, p-JNK1, p-ERK1/2, NF-κB65, p-IκB-α, iNOS, and COX-2 protein expression levels were measured by Western blot. The data from three independent experiments is presented as the mean ± SEM. * $P < 0.05$, ** $P < 0.01$ versus the control group. $P < 0.05$, the LPS (1.5 mg/l) group versus the LPS (1.5 mg/l) group and the LPS (2.0 mg/l) group. $P > 0.05$, the LPS (1.5 mg/l) group versus the LPS (2.0 mg/l) group.

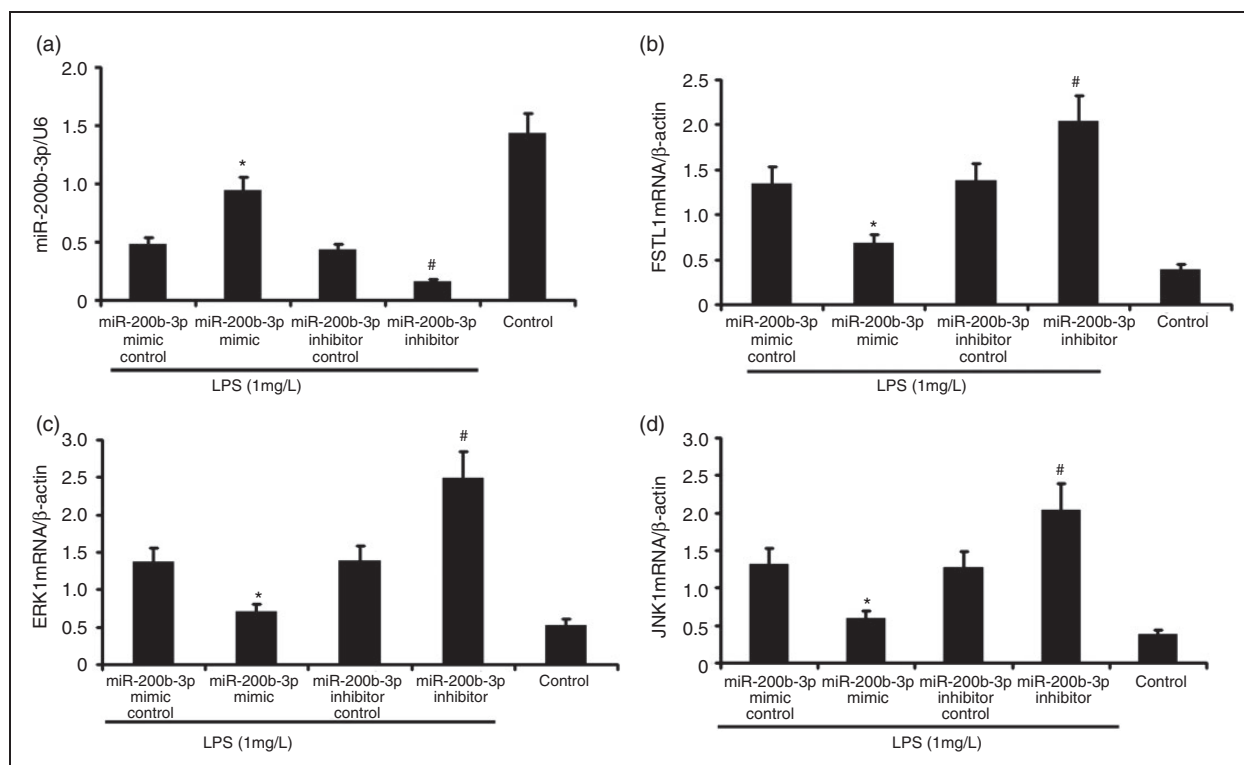


Figure 4. miR-200b-3p mimic increased miR-200b-3p expression and attenuated FSTL1, ERK, and JNK1 mRNA expression in LPS-induced alveolar type II epithelial cells. The A549 cells were transfected with miR-200b-3p mimic and miR-200b-3p inhibitor in the presence of 1 mg/l LPS for 24 h. miR-200b-3p, FSTL1, ERK, and JNK1 mRNA expression in LPS-induced alveolar type II epithelial cells was measured by RT-PCR. The data from three independent experiments is presented as the mean \pm SD. * $P < 0.05$ versus the miR-200b-3p mimic control group. # $P < 0.05$ versus the miR-200b-3p inhibitor control group.

miR-200b-3p overexpression attenuated the inflammation of LPS-induced alveolar type II epithelial cells

The A549 cells were transfected with miR-200b-3p mimic and miR-200b-3p inhibitor in the presence of 1 mg/l LPS for 24 h. PGE2, IL-6, IL-1 β , and TNF- α in A549 cells were measured by ELISA. A549 cell viability was measured by CCK-8. As shown in Figure 5, miR-200b-3p mimic decreased the secretion of PGE2, IL-6, IL-1 β , and TNF- α in A549 cells and increased A549 cell viability. miR-200b-3p inhibitor increased the secretion of PGE2, IL-6, IL-1 β , and TNF- α in LPS-induced A549 cells and increased LPS-induced A549 cell viability.

miR-200b-3p overexpression increased cell viability and survival of LPS-induced alveolar type II epithelial cells

The A549 cells were transfected with miR-200b-3p mimic and miR-200b-3p inhibitor in the presence of 1 mg/l LPS for 24 h. A549 cell survival was measured by MTT, and A549 cell viability was measured by CCK-8. As shown in Figure 6, miR-200b-3p mimic increased

A549 cell viability and survival. miR-200b-3p inhibitor decreased LPS-induced A549 cell viability and survival.

miR-200b-3p overexpression blocked the FSTL1 and ERK/JNK signaling pathway and inflammation of LPS-induced alveolar type II epithelial cells

The A549 cells were transfected with miR-200b-3p mimic and miR-200b-3p inhibitor in the presence of 1 mg/l LPS for 24 h. FSTL1, p-JNK1, p-ERK1/2, NF- κ B65, p-I κ B- α , iNOS, and COX-2 protein expression levels were measured by Western blot. As shown in Figure 7, miR-200b-3p mimic decreased FSTL1, p-JNK1, p-ERK1/2, NF- κ B65, p-I κ B- α , iNOS, and COX-2 protein expression. miR-200b-3p inhibitor increased FSTL1, p-JNK1, p-ERK1/2, NF- κ B65, p-I κ B- α , iNOS, and COX-2 protein expression in LPS-induced A549 cells.

Baicalin increased the expression of miR-200b-3p in LPS-induced alveolar type II epithelial cells

To analyze the effect of LPS on miR-200b-3p expression in A549 cells, we incubated A549 cells with various

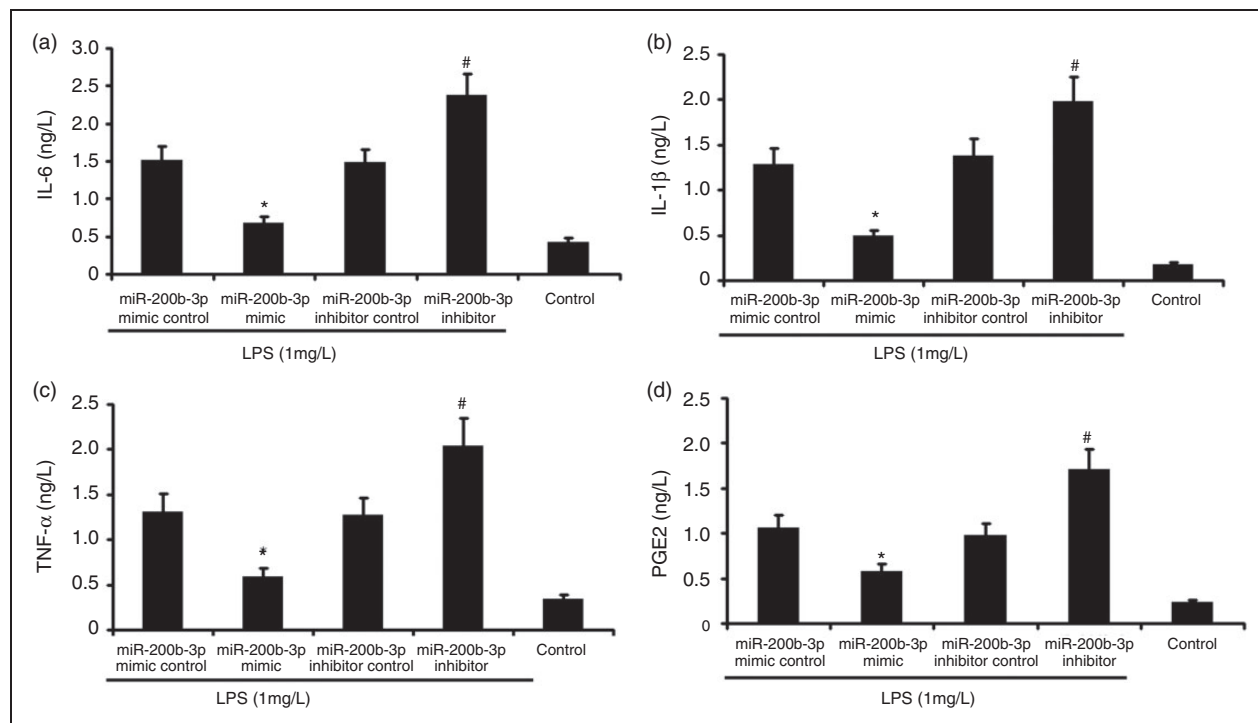


Figure 5. Effect of miR-200b-3p overexpression on the inflammation of LPS-induced alveolar type II epithelial cells. The A549 cells were transfected with miR-200b-3p mimic and miR-200b-3p inhibitor in the presence of 1 mg/l LPS for 24 h. PGE2, IL-6, IL-1 β , and TNF- α in A549 cells were measured by ELISA. The data from three independent experiments is presented as the mean \pm SD. * $P < 0.05$ versus the miR-200b-3p mimic control group. # $P < 0.05$ versus the miR-200b-3p inhibitor control group.

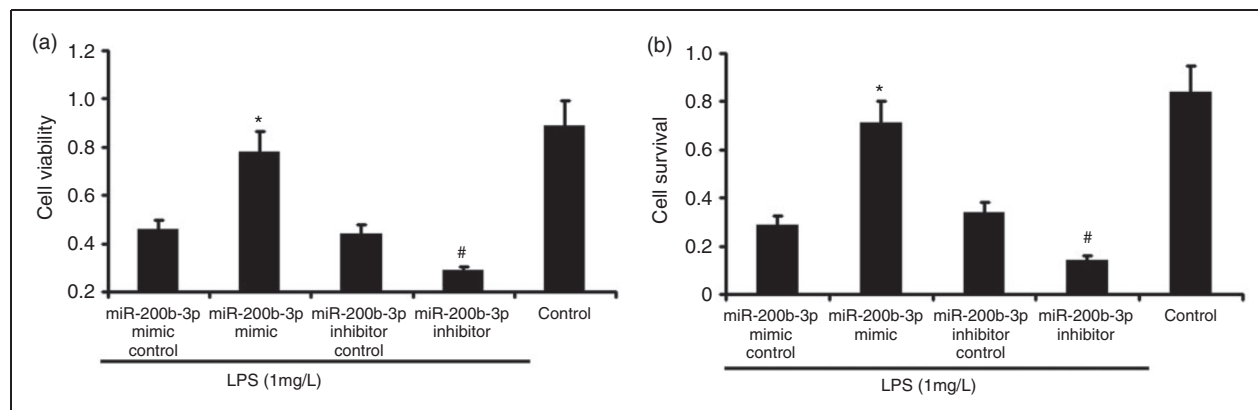


Figure 6. Effect of miR-200b-3p overexpression on the cell survival and viability of LPS-induced alveolar type II epithelial cells. The A549 cells were transfected with miR-200b-3p mimic and miR-200b-3p inhibitor in the presence of 1 mg/l LPS for 24 h. A549 cell survival was measured by MTT. A549 cell viability was measured by CCK-8. The data from three independent experiments is presented as the mean \pm SD. * $P < 0.05$ versus the miR-200b-3p mimic control group. # $P < 0.05$ versus the miR-200b-3p inhibitor control group.

concentrations of LPS (0.5, 1.0, 1.5, and 2.0 mg/l) for 24 h. miR-200b-3p expression was measured by RT-PCR. LPS decreased miR-200b-3p expression in A549 cells in a concentration-dependent manner (Figure 8).

LPS at concentrations as low as 1.0 μ M LPS was effective in decreasing miR-200b-3p expression in A549 cells. To further analyze the effect of baicalin

on the decrease in miR-200b-3p expression by LPS induction in A549 cells, we incubated A549 cells with LPS (1.0 μ M) and various concentrations of baicalin (12.5, 25, 37.5, 50, and 75 μ M) for 24 h. We measured miR-200b-3p expression by RT-PCR and found that baicalin increased miR-200b-3p expression via LPS-induced A549 cells in a concentration-dependent

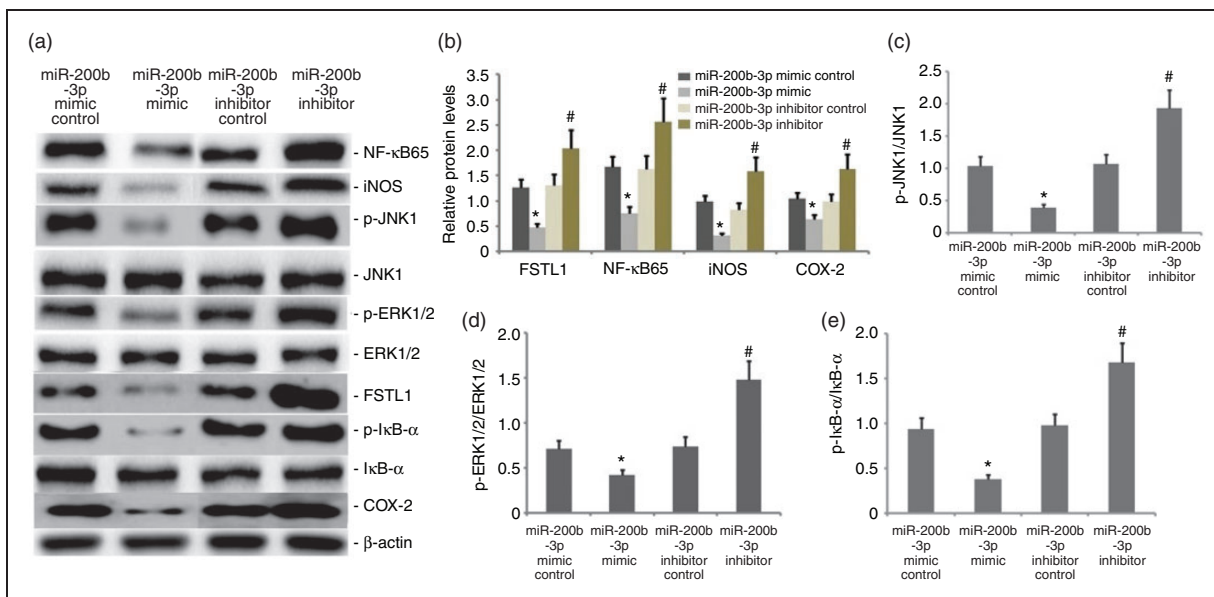


Figure 7. Effect of miR-200b-3p overexpression on the FSTLI and ERK/JNK signaling pathway in the inflammation of LPS-induced alveolar type II epithelial cells. The A549 cells were transfected with miR-200b-3p mimic and miR-200b-3p inhibitor in the presence of 1 mg/l LPS for 24 h. FSTLI, p-JNK1, p-ERK1/2, NF-κB65, p-IκB-α, iNOS, and COX-2 protein expression levels were measured by Western blot. The data from three independent experiments is presented as the mean \pm SD. * P < 0.05 versus the miR-200b-3p mimic control group. # P < 0.05 versus the miR-200b-3p inhibitor control group.

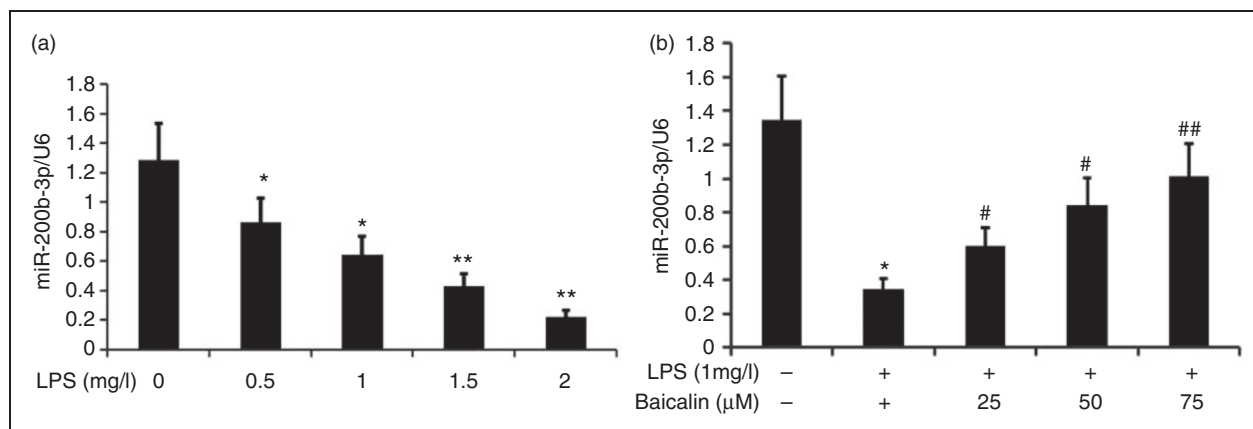


Figure 8. Effect of baicalin on miR-200b-3p expression in LPS-induced A549 cells. A549 cells were incubated with various concentrations of LPS (0.5, 1.0, 1.5, and 2.0 mg/l) or LPS (1.0 mg/l) and various concentrations of baicalin (25, 50, and 75 μ M) for 24 h. miR-200b-3p expression in A549 cells was measured by RT-PCR. The data from three independent experiments is presented as the mean \pm SD. a: * P < 0.05, ** P < 0.01 versus the control group. b: * P < 0.05 versus the control group. # P < 0.05; ## P < 0.01 versus only LPS group. P < 0.05 versus the baicalin (25 μ M) group versus the baicalin (50 μ M) group and the baicalin (75 μ M) group. P > 0.05, the baicalin (50 μ M) group versus the baicalin (75 μ M) group.

manner. Baicalin at concentrations as low as 50 μ M was effective in increasing miR-200b-3p expression in LPS-induced A549 cells.

Baicalin decreased A549 LPS-induced cell inflammation

To observe the effect of baicalin on A549 cell inflammation, we incubated A549 cells with LPS (1.0 mg/l)

and various concentrations of baicalin (25, 50, and 75 μ M) for 24 h. IL-6, PGE2, IL-1 β , and TNF- α in A549 cells were measured by ELISA. Baicalin decreased the secretion of IL-6, PGE2, IL-1 β , and TNF- α in LPS-induced A549 cells in a concentration-dependent manner (Figure 9). Baicalin at concentrations as low as 50 μ M was effective in decreasing IL-6, IL-1 β , PGE2, and TNF- α levels in LPS-induced A549 cells.

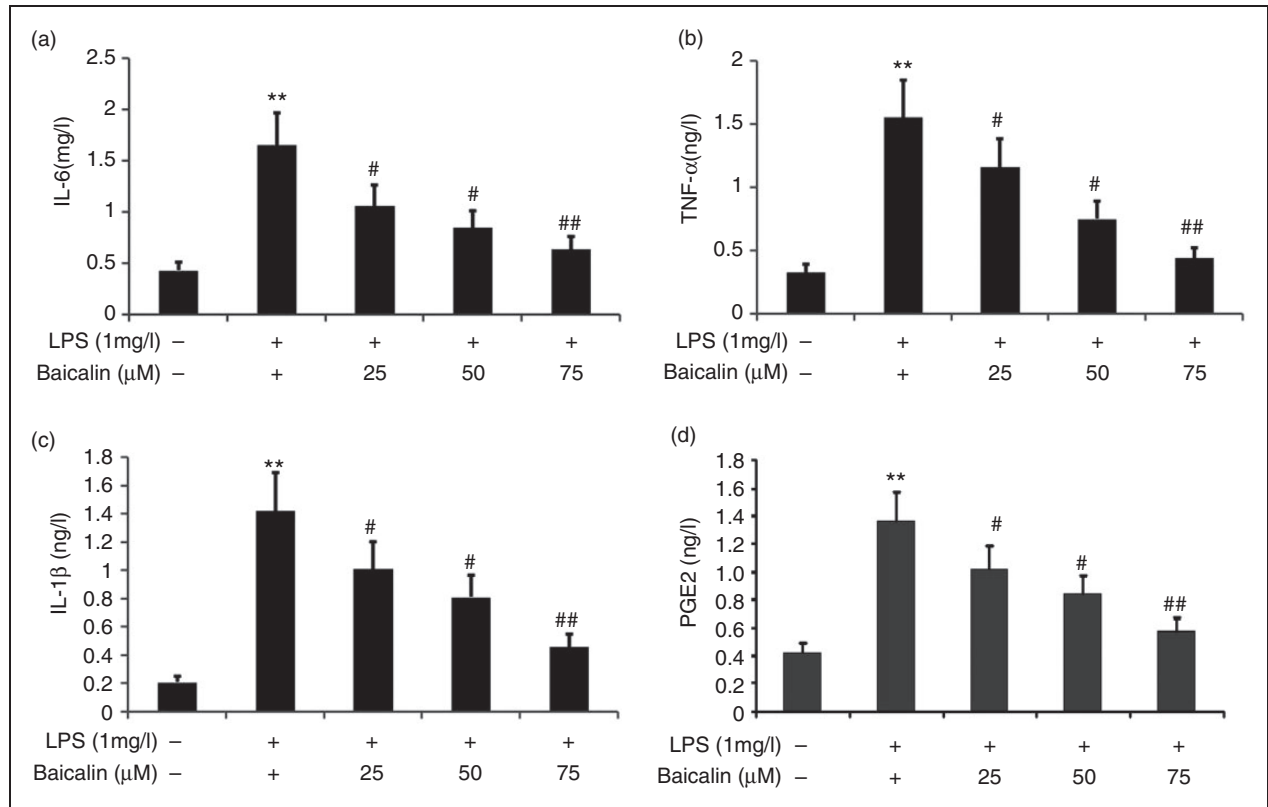


Figure 9. Effect of baicalin on LPS-induced A549 cell inflammation. A549 cells were incubated with LPS (1.0 mg/l) and various concentrations of baicalin (25, 50, and 75 μ M) for 24 h. IL-6, IL-1 β , PGE2, and TNF- α in A549 cells were measured by ELISA. The data from three independent experiments is presented as the mean \pm SD. ** $P < 0.01$ versus the control group. # $P < 0.05$; ### $P < 0.01$ versus only LPS group. $P < 0.05$ versus the baicalin (25 μ M) group versus the baicalin (50 μ M) group and the baicalin (75 μ M) group. $P > 0.05$, the baicalin (50 μ M) group versus the baicalin (75 μ M) group.

Baicalin decreased A549 LPS-induced cell apoptosis

To observe the effect of baicalin on A549 cell inflammation, we incubated A549 cells with LPS (1.0 mg/l) and various concentrations of baicalin (25, 50, and 75 μ M) for 24 h. Baicalin decreased A549 cell apoptosis in a concentration-dependent manner (Figure 10). Baicalin at concentrations as low as 50 μ M was effective in decreasing A549 cell apoptosis LPS-induced A549 cells.

Baicalin increased LPS-induced A549 cell viability and survival rate

To observe the effect of baicalin on A549 cell viability and survival rate, we incubated A549 cells with LPS (1.0 mg/l) and various concentrations of baicalin (25, 50, and 75 μ M) for 24 h. A549 cell viability was measured using CCK-8, and the proliferation rate was measured by MTT assay. Baicalin increased the cell viability and proliferation rate in LPS-induced A549 cells in a concentration-dependent manner (Figure 11). Baicalin at concentrations as low as

50 μ M was effective in increasing the cell viability and proliferation rate in LPS-induced A549 cells.

Baicalin decreased the activity of the FSTL1 and ERK/JNK signaling pathway in LPS-induced alveolar type II epithelial cells

To observe the effect of baicalin on the activity of the FSTL1 and ERK/JNK signaling pathway in LPS-induced A549 cells, we incubated A549 cells with LPS (1.0 mg/l) and various concentrations of baicalin (25, 50, and 75 μ M) for 24 h. FSTL1, p-ERK1/2, p-JNK1, NF- κ B65, p-I κ B- α , iNOS, and COX-2 protein expression levels were measured by Western blot. Baicalin decreased FSTL1, p-ERK1/2, p-JNK1, NF- κ B65, p-I κ B- α , iNOS, and COX-2 protein expression in LPS-induced A549 cells in a concentration-dependent manner (Figure 12). Baicalin at concentrations as low as 50 μ M was effective in blocking the activity of the FSTL1 and ERK/JNK signaling pathway in LPS-induced A549 cells.

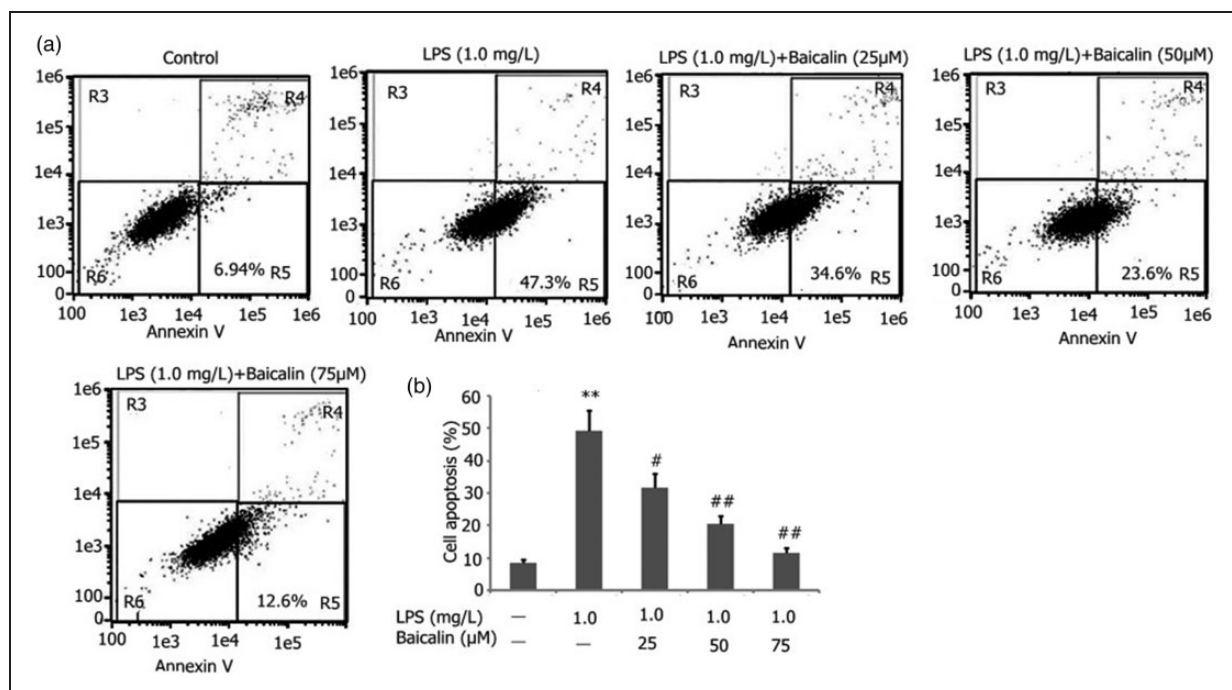


Figure 10. Effect of baicalin on LPS-induced A549 cell apoptosis. A549 cells were incubated with LPS (1.0 mg/l) and various concentrations of baicalin (25, 50, and 75 μ M) for 24 h. A549 cell apoptosis was measured by flow cytometry. The data from three independent experiments is presented as the mean \pm SD. ** $P < 0.01$ versus the control group. # $P < 0.05$; ## $P < 0.01$ versus only LPS group. $P < 0.05$ versus the baicalin (25 μ M) group versus the baicalin (50 μ M) group and the baicalin (75 μ M) group. $P > 0.05$, the baicalin (50 μ M) group versus the baicalin (75 μ M) group.

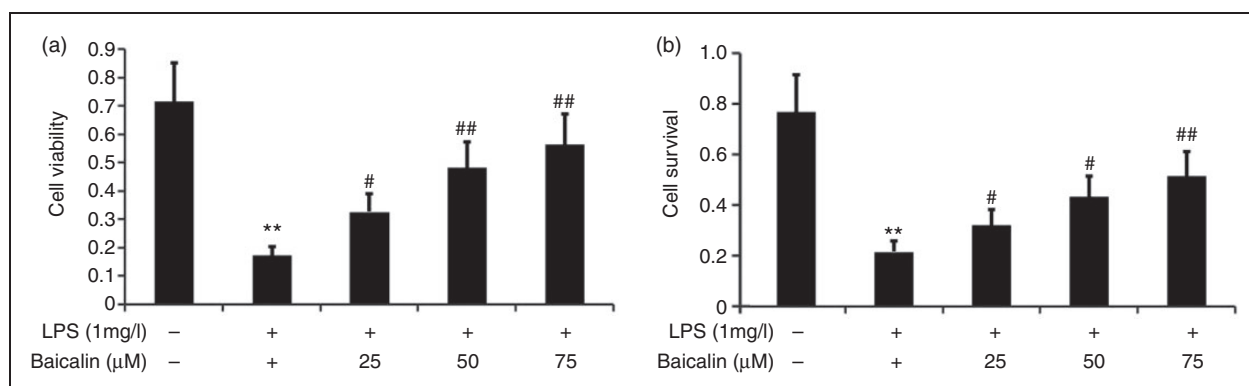


Figure 11. Effect of baicalin on A549 cell viability and survival rate. A549 cells were incubated with LPS (1.0 mg/l) and various concentrations of baicalin (25, 50, and 75 μ M) for 24 h. A549 cell viability was measured using CCK-8, and the proliferation rate was measured by MTT. The data from three independent experiments is presented as the mean \pm SD. ** $P < 0.01$ versus the control group. # $P < 0.05$; ## $P < 0.01$ versus only LPS group. $P < 0.05$ versus the baicalin (25 μ M) group versus the baicalin (50 μ M) group and the baicalin (75 μ M) group. $P > 0.05$, the baicalin (50 μ M) group versus the baicalin (75 μ M) group.

Baicalin combined with miR-200b-3p mimic inhibited the FSTL1 signaling pathway and inflammation in LPS-induced alveolar type II epithelial cells

The A549 cells were transfected with miR-200b-3p mimic in the presence of 1 mg/l LPS and 50 μ M baicalin for 24 h. FSTL1, p-ERK1/2, p-JNK1, NF- κ B65, and p-I κ B- α protein expression levels were measured

by Western blot. Baicalin decreased FSTL1, p-ERK1/2, NF- κ B65, p-JNK1, and p-I κ B- α protein expression in LPS-induced A549 cells in a concentration-dependent manner. IL-6, IL-1 β , and TNF- α in A549 cells were measured by ELISA. Baicalin combined with miR-200b-3p mimic decreased FSTL1, p-ERK1/2, NF- κ B65, p-JNK1, and p-I κ B- α protein expression in LPS-induced A549 cells (Figure 13).

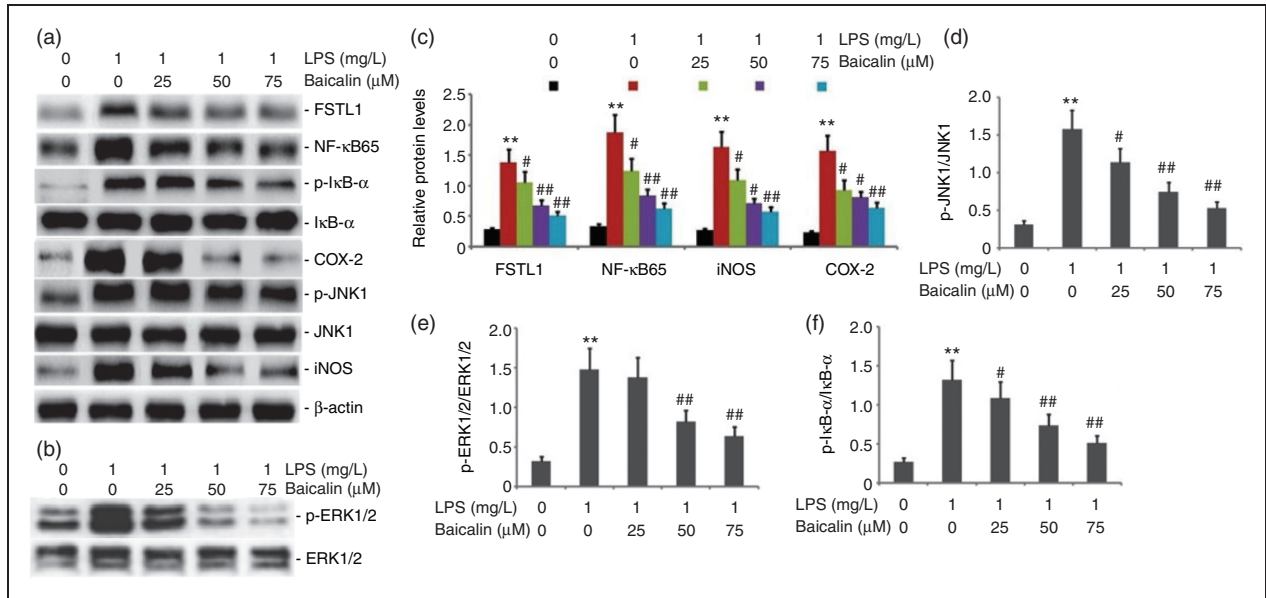


Figure 12. Effect of baicalin on the activity of the FSTLI and ERK/JNK signaling pathway in LPS-induced alveolar type II epithelial cells. A549 cells were incubated with LPS (1.0 mg/l) and various concentrations of baicalin (25, 50, and 75 μM) for 24 h. FSTLI, p-ERK1/2, p-JNK1, NF-κB65, p-IκB-α, iNOS, and COX-2 protein expression levels were measured by Western blot. The data from three independent experiments is presented as the mean ± SEM. ** $P < 0.01$ versus the control group. # $P < 0.05$; ### $P < 0.01$ versus only LPS group. $P < 0.05$ versus the baicalin (25 μM) group versus the baicalin (50 μM) group and the baicalin (75 μM) group. $P > 0.05$, the baicalin (50 μM) group versus the baicalin (75 μM) group. a and b: Representative Western blots of FSTLI, p-ERK1/2, p-JNK1, NF-κB65, p-IκB-α, iNOS, and COX-2 protein expression in LPS-induced alveolar type II epithelial cells. c-f: Statistical summary of the densitometric analysis of FSTLI, p-ERK1/2, p-JNK1, NF-κB65, p-IκB-α, iNOS, and COX-2 protein expression in LPS-induced alveolar type II epithelial cells.

Baicalin combined with miR-200b-3p inhibitor increased LPS-induced A549 cell viability and the survival rate

The A549 cells were transfected with miR-200b-3p inhibitor in the presence of 1 mg/l LPS and 50 μM baicalin for 24 h. A549 cell viability was measured using CCK-8, and the proliferation rate was measured by MTT assay. Baicalin combined with miR-200b-3p mimic increased LPS-induced A549 cell viability and the survival rate in LPS-induced A549 cells (Figure 14).

Baicalin combined with miR-200b-3p inhibitor decreased LPS-induced A549 cell apoptosis and improved LPS-induced A549 cell morphology

The A549 cells were transfected with miR-200b-3p inhibitor in the presence of 1 mg/l LPS and 50 μM baicalin for 24 h. The A549 cell morphology was detected via the AO/EB method. A549 cell apoptosis was measured by flow cytometry. Baicalin combined with miR-200b-3p mimic decreased LPS-induced A549 cell apoptosis. Compared with the control group, the number of adherent cells was significantly reduced, the cells became rounded or branched, some cells were granular

with intact cell membranes but fragile nuclei, and white granular sloughed cells could be observed in the supernatant (Figure 15). Compared with the mimic group, the baicalin combined with miR-200b-3p mimic group had relatively more adherent cells and fewer white granular shed cells (Figure 15).

FSTLI is a regulatory target of miR-200b-3p

We found that FSTLI and miR-200b-3p are important regulators of LPS-induced A549 cell inflammation. To determine how miR-200b-3p regulated LPS-induced A549 cell inflammation, we used TargetScan to predict likely targets of miR-200b-3p. The results revealed that the FSTLI mRNA and protein levels dramatically decreased after miR-200b-3p overexpression, whereas the FSTLI mRNA and protein levels increased after miR-200b-3p down-regulation (Figures 16a and 16b). To validate the interaction between miR-200b-3p and FSTLI, we constructed wild type and mutant FSTLI for a dual luciferase reporter assay (Figures 16c and 16d). As hypothesized, miR-200b-3p bound to the WT FSTLI 3'-UTR but not to the mutant FSTLI 3'-UTR (Figures 16c and 16d).

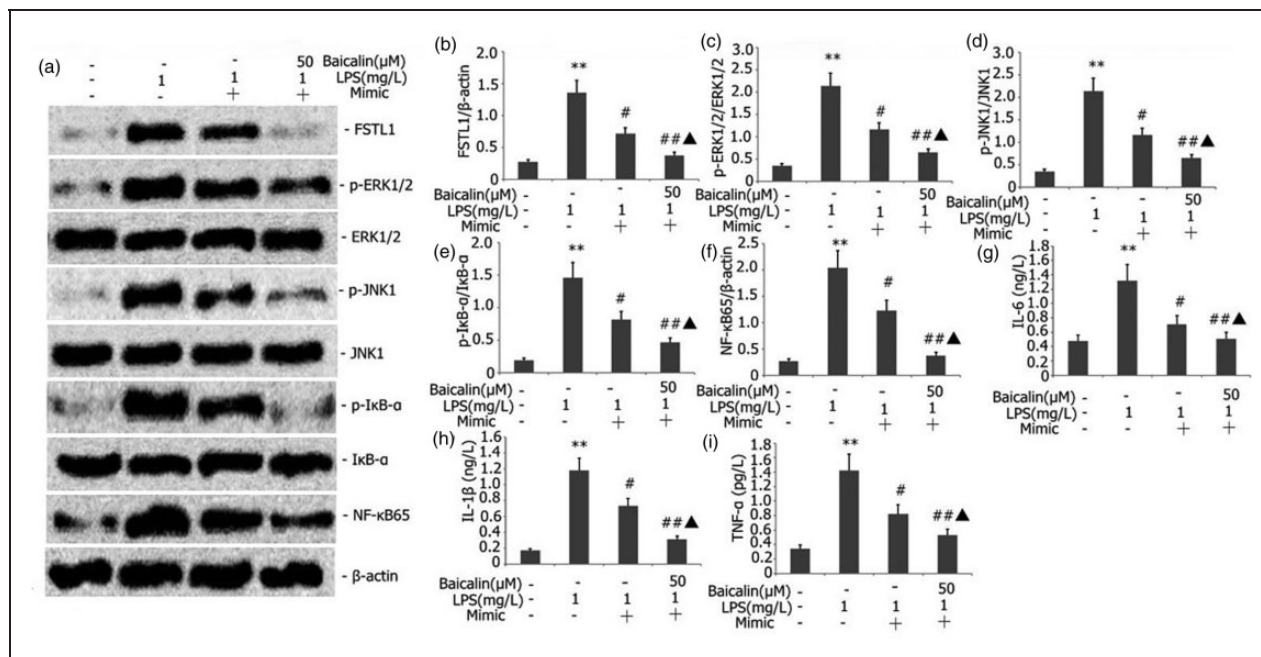


Figure 13. Effect of baicalin combined with miR-200b-3p mimic on the FSTL1 signaling pathway and inflammation in LPS-induced alveolar type II epithelial cells. The A549 cells were transfected with miR-200b-3p mimic in the presence of 1 mg/l LPS and 50 μ M baicalin for 24 h. FSTL1, p-ERK1/2, p-JNK1, NF- κ B65, and p-I κ B- α protein expression levels were measured by Western blot. IL-6, IL-1 β , and TNF- α in A549 cells were measured by ELISA. The data from three independent experiments is presented as the mean \pm SEM. * P < 0.05 versus the control group. # P < 0.05 versus the only LPS group. \blacktriangle P < 0.05 versus the mimic group.

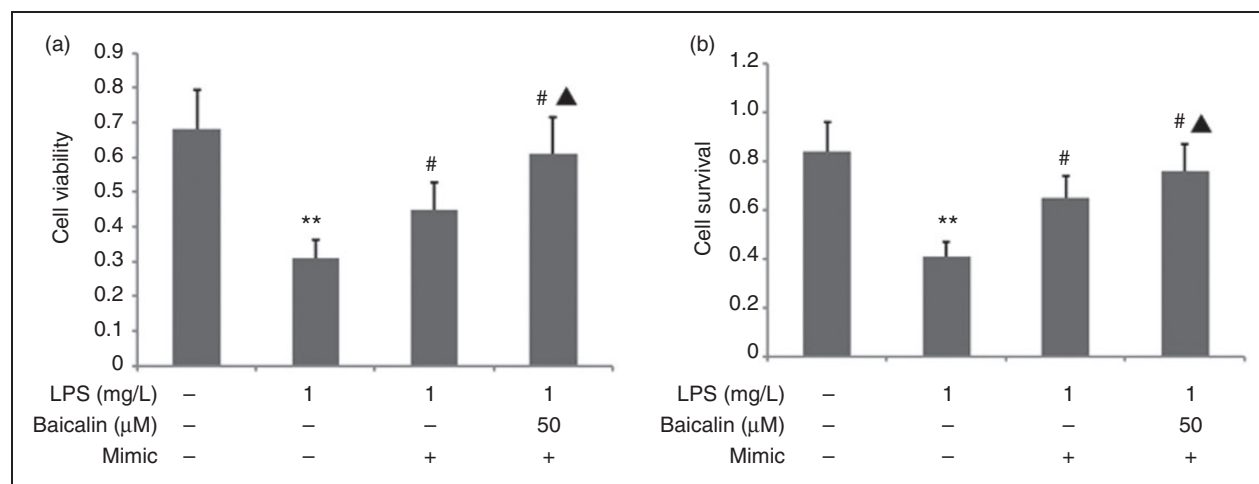


Figure 14. Effect of baicalin combined with miR-200b-3p mimic on LPS-induced A549 cell viability and the survival rate. The A549 cells were transfected with miR-200b-3p inhibitor in the presence of 1 mg/l LPS and 50 μ M baicalin for 24 h. A549 cell viability was measured using CCK-8, and the proliferation rate was measured by MTT assay. The data from three independent experiments is presented as the mean \pm SEM. * P < 0.05 versus the control group. # P < 0.05 versus the only LPS group. \blacktriangle P < 0.05 versus the mimic group.

Correlation between FSTL1 and miR-200b-3p in LPS-induced alveolar type II epithelial cells

We found that FSTL1 mRNA expression decreased in LPS-induced A549 cells transfected with an miR-200b-3p overexpression vector compared with changes from

an empty vector control (P < 0.05; Figure 17). FSTL1 protein expression increased in LPS-induced A549 cells via miR-200b-3p down-regulation (Figure 17).

We further analyzed the correlation between FSTL1 and miR-200b-3p in LPS-induced A549 cells. We found a negative correlation between FSTL1 protein

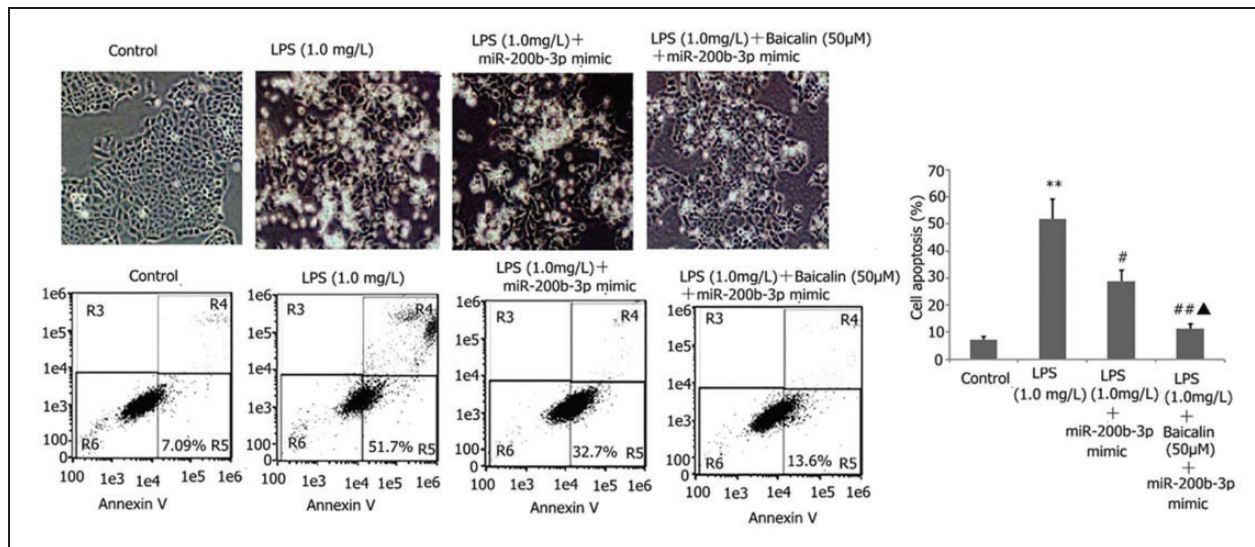


Figure 15. Effect of baicalin combined with miR-200b-3p mimic on LPS-induced A549 cell apoptosis and morphology. The A549 cells were transfected with miR-200b-3p inhibitor in the presence of 1 mg/l LPS and 50 μM baicalin for 24 h. The A549 cell morphology was detected via the AO/EB method. A549 cell apoptosis was measured by flow cytometry. The data from three independent experiments is presented as the mean ± SEM. **P* < 0.05 versus the control group. #*P* < 0.05 versus the only LPS group. ▲*P* < 0.05 versus the mimic group.

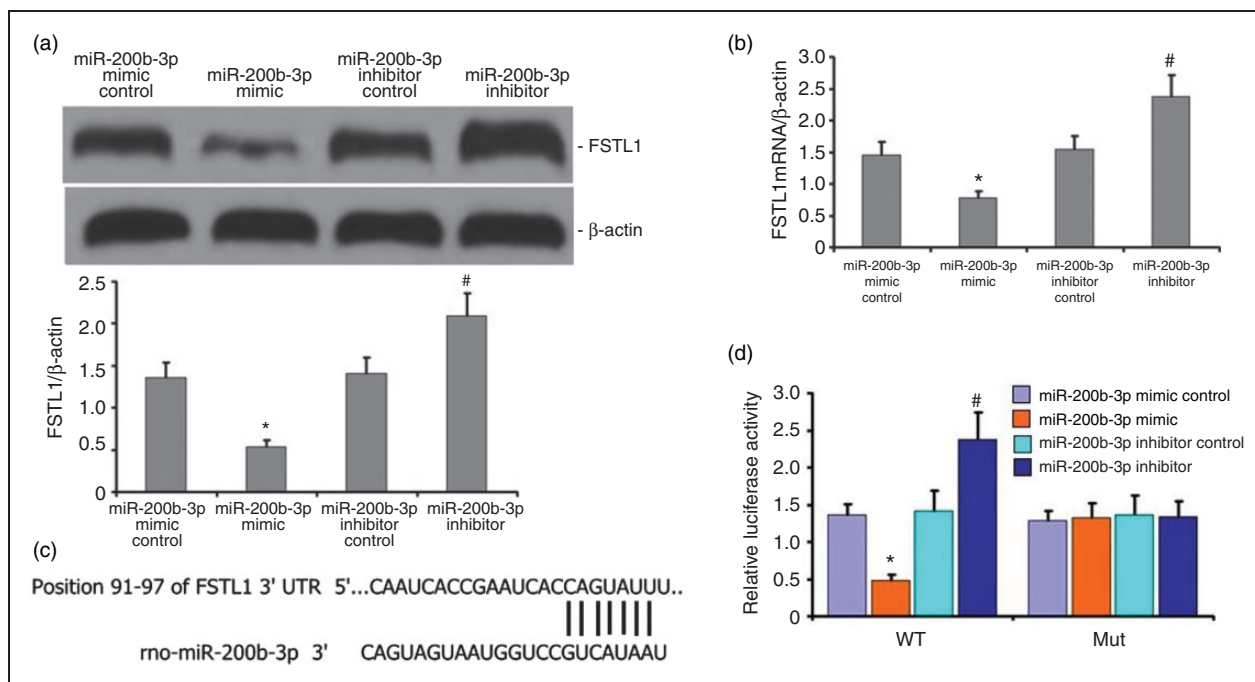


Figure 16. FSTL1 is a downstream target of miR-200b-3p. a and b: FSTL1 decreased in LPS-induced A549 cells with miR-200b-3p overexpression relative to the empty vector control (*P* < 0.05). FSTL1 significantly increased in A549 cells with miR-200b-3p down-regulation. c and d: Decreased mRNA levels of FSTL1 in LPS-induced A549 cells after miR-200b-3p overexpression (*P* < 0.05). Levels were enhanced after miR-200b-3p up-regulation (*P* < 0.05). e, miR-200b-3p was bound to the 3'-UTR regions of FSTL1. Binding was interrupted in mutant FSTL1. f, Dual luciferase reporter assay indicated that the miR-200b-3p mimic was bound to the 3'-UTR region of wild type FSTL1 rather than to FSTL1 mutants (*P* < 0.05).

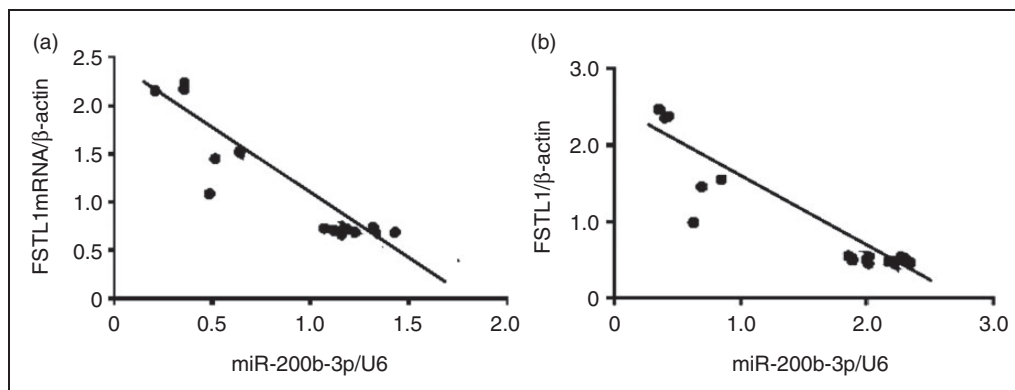


Figure 17. Correlation between FSTL1 and miR-200b-3p in LPS-induced alveolar type II epithelial cells. a and b: Statistical summary of the correlation between mRNA and protein expression of FSTL1 and miR-200b-3p. A negative correlation existed between FSTL1 and miR-200b-3p, as well as between FSTL1 mRNA and miR-200b-3p, in LPS-induced alveolar type II epithelial cells ($r = -0.4588$, $P < 0.05$ and $r = -0.539$, $P < 0.05$, respectively).

and miR-200b-3p, as well as between FSTL1 mRNA and miR-200b-3p, in LPS-induced A549 cells (Figures 17a and 17b).

Discussion

Alveolar epithelial cells (AECs) are the primary target cells attacked by pathogenic endotoxins, as well as inflammatory activated cells and effector cells. They are activated by LPS and the release of inflammatory mediators (such as IL-6, IL-8, TNF- α , intercellular adhesion molecule 1 [ICAM-1], and PGE2), resulting in structural damage, dysfunction, apoptosis, and necrosis of cells.³⁶⁻⁴⁰ A549 cells are widely used in studies on the injury protection mechanism of AECs.⁴¹ Therefore, in this study, we also found that the treatment of A549 cells with endotoxins could cause A549 cells to secrete inflammatory mediators such as IL-6, IL-8, TNF- α , and PGE2. With the increase in endotoxin dosage, the secretion of inflammatory mediators such as IL-6, IL-8, TNF- α , and PGE2 also increased, and the cell activity and cell proliferation of A549 cell decreased. After treatment with baicalin, the secretion of inflammatory mediators such as IL-6, IL-8, TNF- α , and PGE2 decreased, and the cell activity and cell proliferation of A549 cells increased.

Transfection of FSTL1 into macrophages and fibroblasts can lead to the up-regulation of pro-inflammatory cytokines (including IL-1 β , TNF- α , and IL-6).¹⁴ Overexpression of FSTL1 in mouse paws through gene transfer can lead to severe paw swelling and arthritis.⁴² Miyamae et al.⁴² transfected FSTL1 into U937 and COS-7 cells, and a large number of pro-inflammatory factors such as IL-1 β , IL-6, and TNF- α were produced after stimulating with endotoxin and phorbol ester. In addition, injection of adenovirus carrying FSTL1 protein can aggravate joint swelling

and cartilage injury in mice, which might be related to the IFN- γ signaling pathways.⁴² FSTL1 can activate peripheral blood macrophages to secrete a large number of inflammatory factors.⁴² Recent studies have shown that FSTL1 plays an important role in the pathogenesis of bronchial asthma, which can promote airway remodeling and airway inflammation in patients with asthma.⁴¹ The level of FSTL1 in plasma and BALF of patients with asthma was higher than that of the control group, and the increasing degree was positively correlated with airway smooth muscle bundles and thickened reticular basement membrane.⁴³ Proteomic analysis of sputum from patients with asthma showed that FSTL1 was one of the high expression proteins. FSTL1 can also promote airway remodeling in patients with asthma by promoting the autophagy of airway epithelial cells and inducing EMT.⁴⁴ In this study, we further found that the expression of FSTL1 and the secretion of inflammatory mediators increased in A549 cells by inducing A549 cells with endotoxin. By using baicalin to treat LPS-induced A549 cells, we found that the expression of FSTL1 decreased, the inflammation of A549 cells was significantly attenuated, and the activity of A549 cells increased. All these changes suggested that baicalin could reduce the expression of FSTL1 in A549 cells and improve LPS-induced A549 cell inflammation.

MAPKs, including ERK, JNK, and p38MAPK, belong to the serine/threonine protein kinase family; they play an important role in regulating cell proliferation, differentiation, migration, invasion, inflammation, apoptosis, and other biological processes.⁴⁵ ERK1/2 is widely expressed in mammalian cells, and it plays an important role in the regulation of cell mitosis, meiosis, and cell differentiation. After LPS stimulates inflammatory cells, it activates tyrosine protein kinase and induces ERK1/2 phosphorylation through

Raf-1, which leads to a large amount of secreted inflammatory factors (such as IL-1, IL-6, and TNF- α) and increases the expression of iNOS and NO.⁴⁶ JNK is closely related to the inflammatory response. The surface receptors of inflammatory cells recognize external irritants such as endotoxins. After JNK is phosphorylated and activated, two serine residues at the terminals of c-Jun amino, namely, the sites ser63 and ser73, are also phosphorylated. Homologous or heterodimers are recruited to combine with cis-acting elements of the AP-1 gene site to start gene expression of inflammatory cytokines.⁴⁷ In this study, LPS promoted the phosphorylation of ERK1/2 and JNK, resulting in increased ERK/JNK pathway activity and increased A549 cell inflammation. After baicalin treatment, the phosphorylation expression levels of ERK1/2 and JNK decreased, and the ERK/JNK pathway activities were inhibited. Moreover, the endotoxin-induced A549 cell inflammatory response was attenuated. This study also found that FSTL1 could regulate cell and tissue inflammation by regulating ERK/JNK pathway activity. In this study, baicalin could reduce FSTL1, inhibit ERK/JNK pathway activity, and improve LPS-induced A549 cell inflammation.

The miR-200 family, including miR-200a, miR-200b, miR-200c, miR-141, and miR-429, is a family of epithelial cell markers. Among them, miR-200b is an important regulatory factor in EMT progression, which is closely related to the invasion, metastasis, and chemotherapy resistance of tumor cells.⁴⁸ In human lung adenocarcinoma cells, artificial overexpression of miR-200b can inhibit the expression levels of VEGF, Fit-1, and KDR.⁴⁹ In human umbilical vein endothelial cells, overexpression of miR-200b can inhibit VEGF-induced ERK1/2 phosphorylation and the ability of cells to form capillaries in the matrix glue.⁵⁰ Recent studies found that the overexpression of miR-200a can increase nuclear factor erythroid 2-related factor 2 and reduce fructose-induced liver inflammation and oxidative stress by regulating Kelch-like ECH-associated protein 1. miR-200b mimic transfection of high Glc-induced human aortic endothelial cells (HAECs) could reduce the gene expression of ICAM-1, vascular cellular adhesion molecule 1, and E-selectin, as well as decrease the inflammation of high Glc-induced HAECs. In this experiment, in miR-200b-3p mimic-transfected A549 cells, the expression of miR-200b-3p increased; the expression of FSTL1 decreased; the secretion of IL-6, IL-8, TNF- α , PGE2, and other inflammatory mediators in A549 cells decreased; and inflammation was alleviated. The expression of miR-200b-3p increased after treatment with baicalin, thereby inhibiting the

expression of FSTL1 and reducing the inflammation of A549 cells.

NF- κ B is an important pleiotropic nuclear transcription factor, which can specifically bind to the κ B site of various gene promoters to promote transcription expression.⁵¹ Under normal conditions, NF- κ B and I κ B exist in the cytoplasm in the form of a complex. When stimulated by external irritants (such as pathogen invasion), I κ B phosphorylates and then ubiquitinates. Subsequently, it is degraded by proteasome, releasing NF- κ B from the cytoplasm into the nucleus, which binds to DNA. Transcription of binding promoter genes induces the release of inflammatory mediators.⁵² In this experiment, after treatment with baicalin, the activity of NF- κ B/I κ B decreased, and LPS-induced A549 cell inflammation was inhibited.

In this experiment, both miR-200b-3p and FSTL1 could regulate LPS-induced A549 cell inflammation. To clarify the relationship between miR-200b-3p and FSTL1, we predicted that FSTL1 was the regulatory target of miR-200b-3p by TargetScan and confirmed that FSTL1 was the regulatory target of miR-200b-3p through the luciferase reporter assay. These results suggested that miR-200b-3p regulated LPS-induced A549 cell inflammation by regulating the expression of FSTL1.

Baicalin can effectively reduce the proliferation, migration, and apoptosis resistance of pulmonary artery smooth muscle cells induced by hypoxia by up-regulating A2AR and down-regulating the stromal cell-derived factor-1/CXC chemokine receptor 4 axis.⁵³ Baicalin may reduce the level of pro-inflammatory cytokines by regulating the SIRT1 NF- κ B pathway and improve the depression induced by olfactory bulb resection.⁵⁴ Baicalin can also inhibit the NF- κ B and p38 MAPK signaling pathways to achieve anti-fat, antioxidant, and anti-inflammatory effects in a dose-dependent manner; thus, baicalin can improve arteriosclerosis,⁵⁵ inhibit Akt/NF- κ B activation, prevent inflammatory cytokines, and effectively alleviate chronic gastritis.⁵⁶ In this experiment, we found that baicalin could increase the expression of miR-200b-3p, regulate the expression of FSTL1, inhibit the activation of the pro-inflammatory ERK/JNK inflammatory pathway and A549 cell apoptosis, and attenuate LPS-induced A549 cell injury.

In conclusion, this study indicated that miR-200b-3p played an important role in the occurrence and development of endotoxin-induced ALI. Overexpression of miR-200b-3p could regulate the expression of FSTL1, reduce the phosphorylation of ERK1/2 and JNK, inhibit the pathway activity of ERK/JNK, and attenuate the inflammatory response of endotoxin-induced A549 cells. FSTL1 was the regulatory target of miR-200b-3p. Further studies showed that baicalin can

increase the expression of miR-200b-3p, regulate the expression of FSTL1, inhibit the activation of the pro-inflammatory ERK/JNK inflammatory pathway and A549 cell apoptosis, and attenuate the LPS-induced injury of alveolar type II epithelial cells. This experiment revealed the mechanism of baicalin in the treatment of endotoxin-induced ALI and provided the basic theoretical basis for baicalin in treating endotoxin-induced ALI. The mechanism of ALI induced by endotoxin is complicated and unclear, and further research is needed.

Acknowledgements

The authors are grateful to Enpaper for editing the English text of a draft of this manuscript.

Ethics approval and consent to participate

Not applicable.

Patient consent for publication

Not applicable.

Availability of data and materials

The datasets used and/or analyzed in the study are available from the corresponding author upon reasonable request.

Declaration of conflicting interests

The author(s) declared no potential conflicts of interest with respect to the research, authorship, and/or publication of this article.

Funding

The author(s) disclosed receipt of the following financial support for the research, authorship, and/or publication of this article: a grant provided by the National Natural Science Foundation (Grant No. 81960350).

ORCID iD

Ming-wei Liu  <https://orcid.org/0000-0002-3728-2350>

References

- Jain S. Sepsis: An update on current practices in diagnosis and management. *Am J Med Sci* 2018; 356: 277–286.
- Cecconi M, Evans L, Levy M, et al. Sepsis and septic shock. *Lancet* 2018; 392: 75–87.
- Bajwa RPS, Mahadeo KM, Taragin BH et al. Consensus report by pediatric acute lung injury and sepsis investigators and pediatric blood and marrow transplantation consortium joint working committees: supportive care guidelines for management of veno-occlusive disease in children and adolescents, part 1: focus on investigations, prophylaxis, and specific treatment. *Biol Blood Marrow Transplant* 2017; 23: 1817–1825.
- Zheng H, Liang W, He W, et al. Ghrelin attenuates sepsis-induced acute lung injury by inhibiting the NF- κ B, iNOS, and Akt signaling in alveolar macrophages. *Am J Physiol Lung Cell Mol Physiol* 2019; 317: L381–L391.
- Gouda MM and Bhandary YP. Acute lung injury: IL-17A-mediated inflammatory pathway and its regulation by curcumin. *Inflammation* 2019; 42: 1160–1169. d
- D'Alessio FR. Mouse models of acute lung injury and ARDS. *Methods Mol Biol* 2018; 1809: 341–350.
- Peters MMC, Meijs TA, Gathier W, et al. Follistatin-like 1 in cardiovascular disease and inflammation. *Mini Rev Med Chem* 2019; 19: 1379–1389.
- Yang W, Duan Q, Zhu X, et al. Follistatin-like 1 attenuates ischemia/reperfusion injury in cardiomyocytes via regulation of autophagy. *Biomed Res Int* 2019; 2019: 9537382.
- Peters MMC, Meijs TA, Gathier W, et al. Follistatin-like 1 in cardiovascular disease and inflammation. *Mini Rev Med Chem* 2019; 19: 1379–1389.
- Prakash S, Mattiotti A, Sylva M, et al. Identifying pathogenic variants in the Follistatin-like 1 gene (FSTL1) in patients with skeletal and atrioventricular valve disorders. *Mol Genet Genomic Med* 2019; 7: e00567
- Oshima Y, Ouchi N, Sato K, et al. Follistatin-like 1 is an Akt-regulated cardioprotective factor that is secreted by the heart. *Circulation* 2008; 117: 3099–108.
- Kawabata D, Tanaka M, Fujii T, et al. Ameliorative effects of follistatin-related protein/TSC-36/FSTL1 on joint inflammation in a mouse model of arthritis. *Arthritis Rheum* 2004; 50: 660–8.
- Li D, Wang Y, Xu N, et al. Follistatin-like protein 1 is elevated in systemic autoimmune diseases and correlated with disease activity in patients with rheumatoid arthritis. *Arthritis Res Ther* 2011; 13: R17.
- Li D, Wang Y, Xu N, et al. Follistatin-like protein 1 is elevated in systemic autoimmune diseases and correlated with disease activity in patients with rheumatoid arthritis. *Arthritis Res Ther* 2011; 13: R17.
- Wilson DC, Marinov AD, Blair HC, et al. Follistatin-like protein 1 is a mesenchyme-derived inflammatory protein and may represent a biomarker for systemic-onset juvenile rheumatoid arthritis. *Arthritis Rheum* 2010; 62: 2510–6.
- Chaly Y, Fu Y, Marinov A, et al. Follistatin-like protein 1 enhances NLRP3 inflammasome-mediated IL-1 β secretion from monocytes and macrophages *Eur J Immunol* 2014; 44: 1467–79.
- Ni S, Li C, Xu N, et al. Follistatin-like protein 1 induction of matrix metalloproteinase 1, 3 and 13 gene expression in rheumatoid arthritis synoviocytes requires MAPK, JAK/STAT3 and NF- κ B pathways. *J Cell Physiol* 2018; 234: 454–463.
- Song L, Yang H, Wang HX, et al. Inhibition of 12/15 lipoxygenase by baicalein reduces myocardial ischemia/reperfusion injury via modulation of multiple signaling pathways. *Apoptosis* 2014; 19: 567–580.
- Lai CC, Huang PH, Yang AH, et al. Baicalein reduces liver injury induced by myocardial ischemia and reperfusion. *Am J Chinese med* 2016; 44: 531–550.
- Lai CC, Huang PH, Yang AH, et al. Baicalein, a component of *Scutellaria baicalensis*, attenuates kidney injury

- induced by myocardial ischemia and reperfusion. *Planta medica* 2016; 82: 181–189.
21. Sahu BD, Mahesh Kumar J and Sistla R. Baicalein, a bioflavonoid, prevents cisplatin-induced acute kidney injury by up-regulating antioxidant defenses and down-regulating the MAPKs and NF-kappa B pathways. *PLoS one* 2015; 10: e0134139.
 22. Fabian MR, Sonenberg N and Filipowicz W: Regulation of mRNA translation and stability by micro RNAs. *Annu Rev Biochem* 2010; 79: 351–379.
 23. van Leyen K, Kim HY, Lee SR, et al. Baicalein and 12/15-lipoxygenase in the ischemic brain. *Stroke* 2006; 37: 3014–3018.
 24. Saliminejad K, Khorram Khorshid HR, Soleymani Fard S, et al. An overview of microRNAs: biology, functions, therapeutics, and analysis methods. *J Cell Physiol* 2019; 234: 5451–5465.
 25. Zendjabil M, Favard S, Tse C, et al. The microRNAs as biomarkers: what prospects? *C R Biol* 2017; 340: 114–131.
 26. Zou L, Xiong X, Wang K, et al. MicroRNAs in the intestine: role in renewal, homeostasis, and inflammation. *Curr Mol Med* 2018; 18: 190–198.
 27. Danaii S, Shiri S, Dolati S, et al. The association between inflammatory cytokines and miRNAs with slow coronary flow phenomenon. *Iran J Allergy Asthma Immunol* 2020; 19: 56–64.
 28. Möhnle P, Hirschberger S, Hinske LC, et al. MicroRNAs 143 and 150 in whole blood enable detection of T-cell immunoparalysis in sepsis. *Mol Med* 2018; 24: 54.
 29. Zhang X, Gu H, Wang L, et al. MiR-885-3p is down-regulated in peripheral blood mononuclear cells from T1D patients and regulates the inflammatory response via targeting TLR4/NF-κB signaling. *J Gene Med* 2020; 22: e3145.
 30. Lin T, Yu CC, Hsieh PL, et al. Down-regulation of miR-200b-targeting Slug axis by cyclosporine A in human gingival fibroblasts. *J Formos Med Assoc* 2018; 117: 1072–1077.
 31. Ladak SS, Roebuck E, Powell J, et al. The role of miR-200b-3p in modulating TGF-β1-induced injury in human bronchial epithelial cells. *Transplantation* 2019; 103: 2275–2286
 32. Liu J, Wang L and Li X. HMGB3 promotes the proliferation and metastasis of glioblastoma and is negatively regulated by miR-200b-3p and miR-200c-3p. *Cell Biochem Funct* 2018; 36: 357–365.
 33. Cao Y, Liu Y, Ping F, et al. miR-200b/c attenuates lipopolysaccharide-induced early pulmonary fibrosis by targeting ZEB1/2 via p38 MAPK and TGF-β/smad3 signaling pathways. *Lab Invest* 2018; 98: 339–359.
 34. Chen WX, Ren LH and Shi RH. Implication of miRNAs for inflammatory bowel disease treatment: systematic review. *World J Gastrointest Pathophysiol* 2014; 5: 63–70.
 35. Lee KH, Lim BJ, Ferreira VH, et al. Expression of Human miR-200b-3p and -200c-3p in Cytomegalovirus-Infected Tissues. *Biosci Rep* 2018; 38: BSR20180961. https://pubmed.ncbi.nlm.nih.gov/30366960/?from_single_result=miR-200b+and+HCMV&expanded_search_query=miR-200b+and+HCMV-affiliation-3,
 36. Yi X, Wei X, Lv H, et al. Exosomes derived from microRNA-30b-3p-overexpressing mesenchymal stem cells protect against lipopolysaccharide-induced acute lung injury by inhibiting SAA3. *Exp Cell Res* 2019; 383: 111454.
 37. Shen B, Zhao C, Chen C, et al. Picoside II protects rat lung and A549 cell against LPS-induced inflammation by the NF-κB pathway. *Inflammation* 2017; 40: 752–761.
 38. Li D, Cong Z, Yang C, et al. Inhibition of LPS-induced Nox2 activation by VAS2870 protects alveolar epithelial cells through eliminating ROS and restoring tight junctions. *Biochem Biophys Res Commun* 2020; 524: 575–581.
 39. Grazioli S, Dunn-Siegrist I, Pauchard LA, et al. Mitochondrial alarmins are tissue mediators of ventilator-induced lung injury and ARDS. *PLoS One* 2019; 14: e0225468.
 40. Zheng X, Li Q, Tian H, et al. HIP/PAP protects against bleomycin-induced lung injury and inflammation and subsequent fibrosis in mice. *J Cell Mol Med* 2020; 24: 6804–6821.
 41. Shen B, Zhao C, Chen C, et al. Picoside II protects rat lung and A549 cell against LPS-induced inflammation by the NF-κB pathway. *Inflammation* 2017; 40: 752–761.
 42. Miyamae T, Marinov AD, Sowders D, et al. Follistatin-like protein-1 is a novel proinflammatory molecule *J Immunol* 2006; 177: 4758–62.
 43. Liu Y, Liu T, Wu J, et al. The correlation between FSTL1 expression and airway remodeling in asthmatics. *Mediators Inflamm* 2017; 2017: 7918472.
 44. Liu T, Liu Y, Miller M, et al. Autophagy plays a role in FSTL1-induced epithelial mesenchymal transition and airway remodeling in asthma. *Am J Physiol Lung Cell Mol Physiol* 2017; 313: L27–L40.
 45. Zehorai E and Seger R. Beta-like importins mediate the nuclear translocation of MAPKs. *Cell Physiol Biochem* 2019; 52: 802–821.
 46. Zhou LF, Chen QZ, Yang CT, et al. TRPC6 contributes to LPS-induced inflammation through ERK1/2 and p38 pathways in bronchial epithelial cells. *Am J Physiol Cell Physiol* 2018; 314: C278–C288.
 47. Guo M, Härtlova A, Gierliński M, et al. Triggering MSR1 promotes JNK-mediated inflammation in IL-4-activated macrophages. *Embo J* 2019; 38: e100299.
 48. Zhou W, Ye XL, Xu J, et al. The lncRNA H19 mediates breast cancer cell plasticity during EMT and MET plasticity by differentially sponging miR-200b/c and let-7b. *Sci Signal* 2017; 10: eaak9557.
 49. Tang Q, Li M, Chen L, et al. miR-200b/c targets the expression of RhoE and inhibits the proliferation and invasion of non-small cell lung cancer cells. *Int J Oncol* 2018; 53: 1732–1742.
 50. Yang MC, You FL, Wang Z, et al. Salvianolic acid B improves the disruption of high glucose-mediated brain microvascular endothelial cells via the ROS/HIF-1α/VEGF and miR-200b/VEGF signaling pathways. *Neurosci Lett* 2016; 630: 233–240.
 51. DiDonato JA, Mercurio F and Karin M. NF-κB and the link between inflammation and cancer. *Immunol Rev* 2012; 246: 379–400.

52. Zhang L, Zhao J, Gurkar A, et al. Methods to quantify the NF- κ B pathway during senescence. *Methods Mol Biol* 2019; 1896: 231–250.
53. Huang X, Mao W, Zhang T, et al. Baicalin promotes apoptosis and inhibits proliferation and migration of hypoxia-induced pulmonary artery smooth muscle cells by up-regulating A2a receptor via the SDF-1/CXCR4 signaling pathway. *BMC Complement Altern Med* 2018; 18: 330.
54. Yu H, Zhang F and Guan X. Baicalin reverse depressive-like behaviors through regulation SIRT1-NF- κ B signaling pathway in olfactory bulbectomized rats. *Phytother Res* 2019; 33: 1480–1489.
55. Wu Y, Wang F, Fan L, et al. Baicalin alleviates atherosclerosis by relieving oxidative stress and inflammatory responses via inactivating the NF- κ B and p38 MAPK signaling pathways. *Biomed Pharmacother* 2018; 97: 1673–1679.
56. Ji W, Liang K, An R, et al. Baicalin protects against ethanol-induced chronic gastritis in rats by inhibiting Akt/NF- κ B pathway. *Life Sci* 2019; 239: 117064.